Relationship between Regional White Matter Hyperintensities and Alpha Oscillations in Older Adults

Authors: Deniz Kumral, MSc*[1,2], Elena Cesnaite, MSc*[1], Frauke Beyer, PhD[1,3], Simon M. Hofmann, MSc[1], Tilman Hensch, PhD[4,5,6], Christian Sander, PhD[4,5], Ulrich Hegerl, MD[7], Stefan Haufe, PhD[8,9], Arno Villringer, MD[1,2,10], A. Veronica Witte, PhD[1,3,10], Vadim Nikulin, PhD[1,11]

[1]Department of Neurology, Max Planck Institute for Human Cognitive and Brain Sciences, Leipzig, Germany
[2]Berlin School of Mind and Brain, Humboldt-Universität zu Berlin, Berlin, Germany
[3]CRC Obesity Mechanisms, Subproject A1, University of Leipzig, Leipzig, Germany
[4]Department of Psychiatry and Psychotherapy, University of Leipzig Medical Center, Leipzig, Germany
[5]LIFE – Leipzig Research Center for Civilization Diseases, University of Leipzig, Leipzig, Germany
[6]IUBH International University, Erfurt, Germany
[7]Department of Psychiatry, Psychosomatics and Psychotherapy, Goethe University Frankfurt, Frankfurt, Germany
[8]Berlin Center for Advanced Neuroimaging, Charité – Universitätsmedizin Berlin, Berlin, Germany
[9]Bernstein Center for Computational Neuroscience Berlin, Berlin, Germany
[10]Clinic of Cognitive Neurology, University Hospital Leipzig, Leipzig, Germany
[11]Centre for Cognition and Decision Making, Institute of Cognitive Neuroscience, National Research University Higher School of Economics, Moscow, Russian Federation

* These authors contributed equally to the manuscript.

Title character count: 87
Number of figures: 4
Number of tables: 3
Word count abstract: 244
Word count paper:4198

Corresponding Author: Deniz Kumral, Department of Neurology, Max Planck Institute for Human Cognitive and Brain Sciences, Leipzig, Germany, Stephan Str.1a, 04103, Leipzig, Germany

Abstract

Objective

To investigate whether regional white matter hyperintensities (WMHs) relate to alpha oscillations (AO) in a large population-based sample of elderly individuals.

Methods

We associated voxel-wise WMHs from high-resolution 3-Tesla MRI with neuronal alpha oscillations (AO) from resting-state multichannel EEG at sensor (N=907) and source space (N=855) in older participants of the LIFE-Adult study (60–80 years). In EEG, we computed relative alpha power (AP), individual alpha peak frequency (IAPF), as well as long-range temporal correlations (LRTC) that represent dynamic properties of the signal. We implemented whole-brain voxel-wise regression models to identify regions where parameters of AO were linked to probability of WMH occurrence. We further used mediation analyses to examine whether WMH volume mediated the relationship between age and AO.

Results

Higher prevalence of WMHs in the superior and posterior corona radiata was related to elevated relative AP, with strongest correlations in the bilateral occipital cortex, even after controlling for potential confounding factors. The age-related increase of relative AP in the right temporal brain region was shown to be mediated by total WMH volume.

Conclusion

A high relative AP corresponding to increased regional WMHs was not associated with age *per se*, in fact, this relationship was mediated by WMHs. We argue that the WMH-associated increase of AP reflects a generalized and likely compensatory spread of AO leading to a larger number of synchronously recruited neurons. Our findings thus suggest that longitudinal EEG recordings might be sensitive to detect functional changes due to WMHs.

Introduction

White matter lesions (WML) are highly prevalent in the elderly and are of paramount clinical relevance since they are known to accompany cognitive decline and dementia[1–3]. WML are considered to reflect mainly small vessel disease[4], which typically affects periventricular regions and deep white matter sparing U-fibers[1]. Little is known, however, whether and how WML impact functional measures of brain activity. Due to their location, white matter hyperintensities (WMHs) may cause disconnection of neuronal populations[5]. Theoretically, such damage of cortico-cortical and cortico-subcortical pathways is expected to alter synchronized activity of neurons measured with M/EEG[6,7], thus, WML-associated alterations of EEG rhythms seem straightforward. One of the most prominent EEG rhythms are alpha oscillations (AO), which have been shown to originate from thalamo-cortical and cortico-cortical interactions[8,9]. Importantly, measures of AO have been related to many aspects of sensory and cognitive function[10,11].

Although EEG and MRI are recorded daily in a large number of neurological and psychiatric patients all over the world, interestingly, so far only a few studies have investigated the relationship between AO and WML[12–14]. Furthermore, to our knowledge, no direct link between voxel-wise whole-brain WMHs and AO has been investigated. Thus, crucial questions remain unresolved, for example whether changes in AO relate to aging *per se* or rather they represent the impact of age-related neuropathology, for instance, WML.

In this study, using a large population-based sample of elderly individuals, we hypothesized that WMHs affect AO in a topographically specific manner. We further postulated that this effect might be independent of age.

Methods

Participants

Participants were drawn from the population-based Leipzig Research Center for Civilization Diseases LIFE-Adult study[15]. All participants provided written informed consent, and the study was approved by the ethics committee of the medical faculty at the University of Leipzig, Germany. The study was performed in agreement with the Declaration of Helsinki. A subset of participants underwent a 3-Tesla MRI head scan and resting state (rs)EEG recordings on two separate assessment days. We selected participants above 60 years of age and without additional brain pathology or history of stroke, multiple sclerosis, epilepsy, Parkinson's disease, intracranial hemorrhage, or brain tumors. We further excluded individuals whose rsEEG recordings were not temporally close to the MRI acquisition time and participants for whom alpha peak could not be identified. This resulted in a final sample of 907 participants (M=69.49 ± 4.63, 380 female) for the rsEEG sensor space analysis. After excluding individuals with failed T1-weighted segmentation and head-modeling, the final sample for the rsEEG source analysis was 855 (M=68.89 ± 4.66, 360 female). For a detailed overview of the selection process, see Figure 1.

MRI Acquisition and Processing

All MRI scans were performed at 3 Tesla on a MAGNETOM Verio scanner (Siemens, Erlangen, Germany). The body coil was used for radiofrequency (RF) transmission and a 32-channel head coil was used for signal reception. T1-weighted MPRAGE and FLAIR images were acquired as part of a standardized protocol: MPRAGE (flip angle (FA) = 9°, relaxation time (TR) = 2300 ms, inversion time (TI) = 900 ms, echo time (TE) = 2.98 ms, 1-mm isotropic resolution, acquisition time (AT) = 5.10 min); FLAIR (TR = 5000 ms, TI = 1800 ms, TE = 395 ms, 1x0.49x0.49-mm resolution, AT = 7.02 min).

The automated assessment of WMHs was computed in a previous study[16]. All images were checked by a study physician for incidental findings. A computer-based WMHs segmentation algorithm was then used to automatically determine WMH volume on T1-weighted MPRAGE and FLAIR images[17] and inspected visually for segmentation errors. Binary WMH maps of all participants were nonlinearly co-registered to a standardized MNI template (1-mm isometric) with ANTS[18]. In standard space, binary subject-wise WMH maps were grand-averaged to create a population WMH frequency map[19]. As previously implemented[16], to segregate the periventricular (pv)WMH and deep (d)WMH, a default distance of 10 mm to the ventricular surface was used[20]. Every voxel of WMH located within this border was classified as pvWMH; voxels outside the border were classified as dWMH. Regional WMH volume was calculated separately for the deep and periventricular WM. We added a constant value 1 to every participant's regional dWMH volume because there were participants without lesions in the deep WM[16]. We then calculated the ratio of dWMH and pvWMH (dWMH/pvWMH) as localized WMH volume.

EEG Acquisition and Preprocessing

RsEEG activity was recorded in an electrically and acoustically shielded room using an EEG cap with 34 passive Ag/AgCl electrodes (EasyCap, Brain Products GmbH, Germany). 31 scalp electrodes were placed according to the extended international 10–20 system, as shown in Figure 2. The signal was amplified using a QuickAmp amplifier (Brain Products GmbH, Germany). Two electrodes recorded vertical and horizontal eye movements while one bipolar electrode was used for electrocardiography. The rsEEG activity was referenced against common average and sampled at 1000 Hz with a low-pass filter of 280 Hz. Impedances were kept below 10 kΩ. RsEEG data were preprocessed using EEGLAB toolbox (version 14.1.1b) and scripts were custom written in Matlab 9.3 (Mathworks, Natick, MA, USA). We filtered data between 1 and 45 Hz and applied a notch filter at 50 Hz. We then down-sampled the data

to 500 Hz and ran a semi-automatic pipeline for artifact rejection: different noise threshold levels to mark bad time segments were used for the signal filtered in higher frequency (15–45 Hz) and lower frequency (1–15 Hz) ranges. The noise threshold for higher frequencies was set to 40 μV since noise at this range (i.e., induced by muscle activity) is typically lower in amplitude. The noise threshold for the lower frequency range was set to + 3SD over the mean amplitude of a filtered signal between 1 and 15 Hz. To control for the accuracy of automatically marked bad segments, we compared them to the noisy segments marked by another research group[21]. Whenever these segments did not overlap by more than 10 s or they exceeded 60 s of total bad-segment duration, we inspected those datasets visually (~10% of cases) to confirm whether they indeed were contaminated by noise. We further visually assessed power spectral densities (PSD) for data quality and used it to identify broken channels. Next, using independent component analysis (Infomax)[22], activity associated with the confounding sources—namely eye-movements, eye-blinks, muscle activity, and residual heart-related artifacts—was removed.

EEG Sensor Space Analysis

Parameters of Alpha Oscillations

For rsEEG analysis, we used the first 10 min of a recording in order to avoid the potential effect of participants' drowsiness. We individually adjusted the alpha band frequency range by locating a major peak between 7 and 13 Hz on Welch's PSD with 4-s Hanning windows. Thus, we determined individual alpha peak frequency (IAPF) in every channel and defined a bandwidth not exceeding 3 Hz around the peak. We then calculated relative alpha power (AP) for the individually adjusted alpha frequency range dividing it by the broadband power calculated in the 3–45-Hz frequency range. LRTC were calculated using detrended fluctuation analysis on the amplitude envelope (calculated with Hilbert transform) of alpha band oscillations in time windows ranging from 3 to 50 seconds (while respecting the

97 boundaries where the bad segments had been cut) based on the previously published
98 procedure[23]. Here, the scaling exponent (ν) is a measure of the LRTC in the signal. An exponent
99 of 0.5 reflects uncorrelated signals (i.e., resembling white noise), while an exponent between
100 $0.5<\nu<1$ shows persistent autocorrelation and thus the presence of LRTC[23]. The presence of
101 LRTC indicates that past neuronal events are likely to affect neuronal activity in the future even
102 when these events are separated by tens of seconds. The illustration of parameters of AO are
103 shown in Figure 2. To reduce data dimensionality of rsEEG sensor space data used for the
104 whole-brain voxel-wise inference analyses, we further grouped EEG channels into six coarser
105 brain regions (frontal, central, temporal, parietal, and occipital), as shown in Figure 3A.

106 **EEG Source Space Analysis**

107 To reconstruct sources of the rsEEG signal, we calculated leadfield matrices based on
108 individual brain anatomies and standard electrode positions. The T1-weighted MPRAGE
109 images were segmented using the Freesurfer v.5.3.0 software[24]. We constructed a 3-shell
110 boundary element model (BEM) which was subsequently used to compute the leadfield matrix
111 using OpenMEEG[25]. Approximately 2,000 cortical dipolar sources were modeled for each
112 individual. Source reconstruction was performed using exact low resolution brain
113 electromagnetic tomography (eLORETA)[26] with a regularization parameter of 0.05. We
114 filtered the signal within the individually adjusted alpha frequency band range as well as in
115 broadband range (3–45 Hz), squared it, and summed up across all three dipole directions.
116 Relative AP was then calculated in each voxel through the division of AP by the broadband
117 power. The cortex surface mantle was divided into 68 regions of interest (ROIs) based on the
118 Desikan-Killiany atlas[27]. These were further combined into five coarser ROIs (frontal, parietal,
119 temporal, occipital, and cingulate) for the right and left hemispheres following a standard
120 parcellation atlas, as shown in Figure 3B. Relative AP values were averaged across each ROI.

Statistical Analyses

Correlation of Age with WMH Volume and Alpha Oscillations

Pearson correlations were calculated to examine the relationship between i) age and total and regional WMH volume (dWMH/pvWMH) and ii) the parameters of AO in six regions at sensor space. Differences between correlations were assessed with Fisher's r-to-z transformation implemented in R version 3.5.2 (http://www.R-project.org/). To correct for multiple comparisons, p-values were then adjusted using the False Discovery Rate (FDR)[28].

Topographical Relevance Analyses of WMHs for Alpha Oscillations at Sensor Space

To identify regions in which WMHs robustly correlated with AO, we performed whole-brain voxel-wise regressions. More precisely, we applied general linear models (GLMs) in which individual values of IAPF, relative AP, and LRTC were used as predictors for the topographical occurrence of WMHs, adjusting for effects of age, sex, and intracranial volume (ICV) as covariates of no interest. 3D voxel-wise binary lesion maps were analyzed using FSL's randomize[29]. For each statistical analysis, positive and negative contrasts were computed. Significance of results was based on threshold-free cluster enhancement (TFCE, N=10,000 permutations) with family-wise error (FWE) corrected p-values of $p<0.05$. We further reported statistical results for the more conservative FWE threshold of $p<0.005$.

Topographical Relevance Analyses of WMHs for Alpha Power at Source Space

To assess the association between relative AP and whole-brain WMHs, we implemented GLMs separately for 10 ROIs with relative AP as covariate of interest, and age, sex, and ICV as covariates of no interest. Because we found a positive correlation between the voxel-wise occurrence of WMHs and relative AP at the sensor space, we only computed a positive contrast. All statistical analyses were further corrected for multiple comparisons using

144 TFCE based permutation testing (N=10,000) at FWE level of $p<0.05$, as well as with a
145 conservative threshold of $p<0.005$.

146 *Sensitivity Analyses*

147 *Control for Confounding factors.* Given that different cardiovascular risk factors
148 including body mass index (BMI), systolic blood pressure (SBP), smoking, and diabetes are
149 associated[1,16,30] WMH[3,17,31], we further considered these factors as potential confounders (as
150 covariates of no interest) for the voxel-wise associations between parameters of AP and
151 probability of WMH occurrence in the overall sample (N=907). To assess a degree of
152 collinearity between the regressors used in GLMs, we additionally computed variance inflation
153 factor (vif) in R. All predictors had a vif score below 2, therefore, we concluded that models
154 showed acceptably low multicollinearity.

155 *Medication*. We implemented the voxel-wise inference analyses between parameters of
156 AO and WMHs excluding participants taking medications affecting the central nervous system
157 (opioids, hypnotics and sedatives, anti-parkinsonian drugs, anxiolytics, anti-psychotics, anti-
158 epileptic drugs). The resulting sample included 801 individuals ($M = 68.96 \pm 4.58$, 323 female).

159 *Control Analyses*. To assess the robustness of our results, we further applied voxel-wise
160 inference analyses between the probability of WMH occurrence and absolute AP in the left and
161 right occipital region at EEG source space, using age, sex, and ICV as covariates of no interest.
162 Absolute EEG power in both regions was log transformed to normalize the distribution of the
163 data for statistical analyses.

164 **Mediation Analyses**

165 We performed mediation analyses using *mediation* package[31] in R to examine whether
166 total or localized WMH (dWMH/pvWMH) volume mediates the relationship between age as

an independent and AO at sensor space as a dependent variable. We computed 99% confidence intervals (CI) using bootstrapping (5,000) for all inferences. Indirect effects, and the sum of the indirect effects were considered significant if the CI did not contain zero. Here, direct and mediation effects are called average direct effect (ADE) and average causal mediation effect (ACME, also referred to as indirect effect), respectively. Statistically, total effect is the sum of ACME and ADE. The ACME shows whether age was associated with parameters of AO through a mediator.

Data availability

Supplementary data can be found in the open science framework (OSF; https://osf.io/mdwc6/) Anonymized data will be made available upon request through the application procedure carried out by the LIFE-Study administration (https://life.uni-leipzig.de/de/erwachsenen_kohorten/life_adult.html).

Results

Sample Characteristics

Details about the demographic, anthropometric, cardiovascular measures, as well as WMH volume, and AO can be found in *Table 1*.

Topography and Characteristics of Alpha Oscillations

The relative AP at sensor space showed a maximum over the occipital channels, with a mean value of 0.66 ± 0.17. Similarly, the relative AP at source space showed a maximum over the bilateral occipital cortex, including cuneus and lateral occipital regions with a mean value of 0.59 ± 0.18. The grand-average IAPF was 9.40 ± 0.49 Hz, showing larger values at occipital regions. The average scaling exponent (v) was 0.72 ± 0.017. Similarly, topographies of the scaling exponent had higher values at occipital and parietal areas as well as frontal regions.

Correlations

Association of Age with WMH Volume and Alpha Oscillations

We found a correlation between age and total WMH volume ($r=0.374$, $p<0.001$), but not with the dWMH/pvWMH ($p>0.05$). Regarding parameters of AO, we found that higher age was associated with decreased IAPF in all EEG ROIs (r from -0.13 to -0.17, $p_{FDR}<0.05$), while no correlations between age and relative AP or LRTC were found (all $p_{FDR}>0.05$).

Topographical Association Between WMHs and Alpha Oscillations at Sensor Space

The voxel-wise inference analyses revealed that higher relative AP in the frontal region was correlated with higher WMH probabilities in the right body of corpus callosum ([16, -26, 32], T=3.76, k=653). Higher relative AP in the central region was associated with higher WMH probabilities in the right anterior thalamic radiation extending to the posterior corona radiata ([22, -49, 37], T = 4.44, k=2,744), while higher relative AP in the right temporal region

202 was linked to higher WMHs in the right superior longitudinal fasciculus ([22, -49, 37], T=4.52,
203 k=6,893) extending to the left inferior fronto-occipital fasciculus ([-21, -53, 32], T=4.00,
204 k=4,210). Furthermore, higher relative AP in the parietal region was associated with higher
205 WMHs in the right superior corona radiata ([18, -19, 37], T=4.05, k=4,474). Similarly, for
206 relative AP in the occipital region, we observed a higher prevalence of WMHs in the bilateral
207 superior corona radiata through the body of the corpus callosum to the anterior corona radiata,
208 including the right anterior thalamic radiation ([18, -19, 37], T=4.39, k=9,450). Accordingly,
209 higher voxel-wise WMH probabilities were associated with higher relative AP independent of
210 age, sex, and brain size, as shown in Figure 4A and 4B. Note that using a more stringent FWE
211 rate of $p < 0.005$, correlation between probability of WMH occurrence and relative AP was
212 only evident for the occipital region ([18, -19, 37], T=4.39, k=904). Finally, no associations
213 between voxel-wise WMHs and IAPF or LRTC were observed ($p>0.05$).

214 *Topographical Association Between WMHs and Alpha Oscillations at Source Space*

215 We found that higher relative AP in all EEG regions except for the left frontal region
216 was associated with higher probability of WMH occurrence (*Table 2*). With the stricter FWE-
217 level of $p<0.005$, the association between the occurrence of WMHs and relative AP was
218 evident for left ([18, -19, 37], T=4.29, k=192) and right occipital regions ([18, -19, 37],
219 T=4.45, k=845).

220 *Sensitivity Analyses*

221 *Control for Confounding Factors.* Voxel-wise inference analyses after controlling for
222 age, sex, ICV, BMI, SBP, diabetes, and smoking status yielded a similar relationship between
223 higher WMH probability and elevated relative AP in the following regions: central ([22, -49,
224 37], T=4.46, k=5417), right temporal ([22, -49, 37], T=4.52, k=5,417), left temporal ([22, -
225 49, 37], T=4.59, k=4772), parietal ([18, -19, 37], T=3.68, k=231), and occipital ([18, -19,

226 37], T=4.08, k=4,018) EEG regions across the overall sample. Note that with TFCE, FWE-
227 corrected, p<0.005, we did not find any clusters. Lastly, no WMH clusters were related to
228 IAPF or LRTC (p>0.05).

229 *Medication.* Voxel-wise inference analyses excluding individuals taking central
230 nervous system medication still indicated the association between higher prevalence of WMHs
231 and increased relative AP at sensor space in the following regions: frontal ([17, 9, 31], T=4.42,
232 k=6,880), central ([20, -30, 35], T= 4.46, k=9,063), right temporal ([20, -48, 35], T=4.57,
233 k=12,098), left temporal ([22, -49, 37], T=4.61, k=9,408), parietal ([14, -8, 31], T=4.61,
234 k=9,054), and occipital ([18, -19, 37], T=4.44, k=12,885) EEG regions. Importantly, with
235 TFCE, FWE-corrected, p<0.005, we identified WMHs clusters (k>2,000) for occipital, left
236 temporal, right temporal, and a small cluster (k>200) for parietal and central EEG regions.
237 Additional voxel-wise inference analyses revealed that higher WMHs resulted in decreased
238 IAPF in right temporal ([17, -27, 33], T=4.00, k=138) and left temporal regions ([17, -27,
239 33], T=4.12, k=503). Lastly, no WMHs clusters were related to LRTC (p>0.05).

240 *Control Analyses.* Voxel-wise inference analyses with absolute AP similarly indicated
241 that higher probability of WMH occurrence was associated with elevated absolute AP in right
242 ([-23, 0, 36], T=3.98, k=5,633) and left occipital regions ([-23, 0, 36], T=4.05, k=5,358).

243 **Mediation Analyses**

244 We examined whether a total or localized (dWMH/pvWMH) WMH volume could
245 mediate the relationship between age and relative AP, IAPF, and LRTC in all ROIs.
246 Investigating the relationship between age and relative AP, we observed a significant indirect
247 effect (i.e., ACME) of total WMH volume, while ADE and total effect were not significant for
248 most of the regions (99% |CI| > 0, Table 3). Only in the right temporal region at sensor space
249 did the total effect of age on relative AP appear to be significant (p<0.05), indicating specific

pathways between age and relative AP through total WMH volume. Further, we confirmed the indirect effects of total WMH volume for relative AP at EEG source space for left parietal (β=0.0012, CI = [0.00006-0.002]), left (β=0.0014, CI = [0.00013-0.002]) and right occipital (β=0.0014, CI = [0.00015-0.0028]) regions. Finally, our results further revealed that neither total nor localized WMH volume mediated the association of age with IAPF and LRTC at sensor space (all $p>0.05$).

Discussion

The main goal of this study was to investigate whether regional WMHs affect parameters of alpha oscillations independently from age. We pursued this aim using a large sample of healthy older individuals from a population-based study[15]. We showed distinct regional relationships between relative AP and WMHs: our topographical analysis suggested that higher occurrence of WMHs in superior, posterior to anterior corona radiata through the body of corpus callosum was related to higher relative AP, with strongest correlations in the bilateral occipital cortex. Adjusting for potential confounding factors including age and cardiovascular risk factors did not change these results.

Alpha rhythm is the most salient rsEEG oscillatory phenomenon that originates from thalamo-cortical and cortico-cortical interactions[8,9]. Alterations in AO have previously been linked to changes in different anatomical and metabolic features including properties of WM (e.g., fractional anisotropy measured by diffusion tensor imaging)[7], amount of cerebrospinal fluid[32], and cerebral glucose metabolism[33]. Regarding WMHs, for instance, a previous EEG-MRI study showed that higher relative AP in parietal regions was associated with higher scores of the prevalence of WMLs in 79 individuals with mild cognitive impairment[14], consistent with our findings in this population-based sample. Previous studies with computational models have given further support for the notion that resonance properties of feedforward, cortico-thalamo-cortical, and intra-cortical circuits largely influence AO[6]. In the present study, we similarly observed that regional WMHs, detected mostly in superior corona radiata, containing thalamo-cortical fibers, affect inter-individual differences in relative AP. Since damage to fibers of the superior corona radiata—connecting the basal ganglia and thalamus to the superior frontal gyrus—is known to be associated with cognitive dysfunction[34], it is likely that such an elevated AP may be triggered to recruit compensatory neuronal resources to maintain cognitive functioning. But, how could lesions in the WM possibly affect EEG signal which mainly

281 reflects neural synchrony within gray matter? While in principle a hyperintensity in T2-
282 weighted MR sequences is a quite unspecific marker of various pathologies, postmortem
283 histopathological studies of elderly subjects with WML have mostly reported demyelination,
284 axonal loss, and other consequences of ischemic small vessel disease[4,35]. Myelin contributes to
285 the speed of impulse conduction through axons, and the synchrony of impulses between distant
286 cortical regions[36,37]. Reductions of conduction velocity due to demyelination and loss of
287 (communicating) axons are assumed to be responsible for cognitive dysfunctions which are
288 known to be based on delicately orchestrated propagations of neuronal signals.
289 Electrophysiologically, interactions and synchrony between neuronal populations are reflected
290 in rhythmic M/EEG signals, of which AO are the most prominent ones[8,9]. AP is a quantitative
291 marker of the degree of synchrony in the neuronal activity of the corresponding neuronal
292 populations[38]. While for a long-time AO were regarded as idle rhythms of non-active brain
293 areas, a plenitude of studies has convincingly demonstrated that AO play an important role in
294 many cognitive functions[10,11]. For instance, in motor and sensory domains it has been shown
295 that amplitude decreases of AO in focal areas (i.e., reflecting cortical activation) is in turn
296 associated with the inhibition of neighboring cortical areas. This phenomenon is thought to
297 result from a reciprocal relationship between thalamo-cortical and reticular nucleus cells on
298 which the generation of AO is based[39]. Such topographically specific relationships are likely
299 to be disturbed by alterations in conduction velocity and axonal loss in the thalamo-cortical
300 circuitry. A consequence is a less precise and more generalized (i.e., compensatory) spread of
301 AO across the cortex leading to a larger number of synchronously recruited neurons and
302 correspondingly to larger AP. This in turn might explain a positive association between AP and
303 WMH.

304 In our study, we did not find strong evidence for age-related attenuations of relative AP,
305 in line with other recent studies[40,41]. This could be due to the narrow age range of our

306 participants, as well as the individually adjusted alpha frequency range based on the IAPF. In
307 fact, preserved peak power at IAPF has recently been reported in an older sample[41], suggesting
308 that any observed age-dependent power changes might be due to shifts in the frequency range
309 at which alpha peak occurs. Noteworthy, mediation analysis in the current study indicated that
310 the influence of higher age to elevated relative AP (in the right temporal region) was mediated
311 by the higher total WMH volume.

312 In the literature, other commonly reported age-dependent changes in spectral
313 parameters of EEG include slowing of the alpha peak[42]. We replicated the slowing of the IAPF
314 with increasing age despite the narrow age range. Alpha peak slowing has previously been
315 suggested to be linked to a less efficient coordination of neuronal activity in this frequency
316 range[43]. We further explored the relationship between age and LRTC in the amplitude envelope
317 of AO that represents scale-free modulation of resting state oscillations. LRTC have previously
318 been linked to the presence of a critical state in neural networks, which is characterized by the
319 balance of excitation and inhibition[44]. Regarding the association between age and LRTC,
320 previous studies have shown that the observed age-related changes might be dependent on age
321 range—it increases from childhood to early adulthood, after which it stabilizes[45,46]. In
322 accordance with these previous findings, in our sample of elderly subjects we observed no
323 pronounced age-related LRTC attenuations, which is consistent with relatively stable dynamic
324 properties of neuronal oscillations at higher age.

325 While a strength of this study is in the large population-based sample, one of the
326 limitations is in investigating only *cortical* oscillations. An interesting direction for future
327 research would be to study generators of oscillations in deep brain structures (e.g., thalamus)
328 and how they propagate through WM pathways, especially when these pathways are affected.
329 Research using other advanced techniques such as quantitative MRI or specific assessment of
330 tissue properties with ultra-high field MRI combined with intracranial EEG recording could

further provide valuable insights into the nature of the relationship between WM properties and AO. Lastly, we performed a relatively coarse parcellation of the brain at EEG source space analysis due to the relatively small number of electrodes (n=31). A denser spatial sampling of the EEG (not available in the present cohort) would allow investigation of this relationship with better spatial precision.

In conclusion, using sensitive high-resolution neuroimaging techniques, we showed that elevated relative AP is related to higher probability of WMHs, supporting the idea that damage to WM may lead to compensatory enhancement of rhythmic activity in the alpha frequency range. Importantly, our study provides evidence that the prevalence of regional WMHs, characterized by higher relative AP, was not associated with age *per se*, in fact, the latter seems to be mediated by total WMH volume. Our findings thus suggest that longitudinal EEG recordings might be sensitive for the detection of alterations in neuronal activities due to progressive structural changes in WM.

Acknowledgments

We thank all members of the Leipzig Research Center for Civilization Diseases (LIFE) study center for conducting the LIFE-Adult study and also all participants for their valuable collaboration.

Funding

This work is supported by the European Union, the European Regional Development Fund, and the Free State of Saxony within the framework of the excellence initiative and LIFE – Leipzig Research Center for Civilization Diseases, University of Leipzig.

SH is funded by the European Research Council (ERC) under the European Union's Horizon 2020 research and innovation programme (Grant agreement No. 758985).

References

1. Habes M, Erus G, Toledo JB, et al. White matter hyperintensities and imaging patterns of brain ageing in the general population. *Brain*. 2016;139(4):1164-1179. doi:10.1093/brain/aww008
2. Debette S, Markus HS. The clinical importance of white matter hyperintensities on brain magnetic resonance imaging: Systematic review and meta-analysis. *BMJ*. 2010;341(7767):288. doi:10.1136/bmj.c3666
3. Maillard P, Carmichael O, Fletcher E, Reed B, Mungas D, DeCarli C. Coevolution of white matter hyperintensities and cognition in the elderly. *Neurology*. 2012;79(5):442-448. doi:10.1212/WNL.0b013e3182617136
4. Wardlaw JM, Valdés Hernández MC, Muñoz-Maniega S. What are white matter hyperintensities made of? Relevance to vascular cognitive impairment. *J Am Heart Assoc*. 2015;4(6):001140. doi:10.1161/JAHA.114.001140
5. O'Sullivan M, Jones DK, Summers PE, Morris RG, Williams SCR, Markus HS. Evidence for cortical "disconnection" as a mechanism of age-related cognitive decline. *Neurology*. 2001;57(4):632-638. doi:10.1212/WNL.57.4.632
6. Hindriks R, van Putten MJAM. Thalamo-cortical mechanisms underlying changes in amplitude and frequency of human alpha oscillations. *Neuroimage*. 2013;70:150-163. doi:10.1016/j.neuroimage.2012.12.018
7. Valdés-Hernández PA, Ojeda-González A, Martínez-Montes E, et al. White matter architecture rather than cortical surface area correlates with the EEG alpha rhythm. *Neuroimage*. 2010;49(3):2328-2339. doi:10.1016/j.neuroimage.2009.10.030
8. Bazanova OM, Vernon D. Interpreting EEG alpha activity. *Neurosci Biobehav Rev*. 2014;44:94-110. doi:10.1016/J.NEUBIOREV.2013.05.007
9. Lopes Da Silva FH, Pijn JP, Velis D, Nijssen PCG. Alpha rhythms: Noise, dynamics and models. *Int J Psychophysiol*. 1997;26(1-3):237-249. doi:10.1016/S0167-8760(97)00767-8
10. Fox NA, Yoo KH, Bowman LC, et al. Assessing human mirror activity With EEG mu rhythm: A meta-analysis. *Psychol Bull*. 2016;142(3):291-313. doi:10.1037/bul0000031
11. Klimesch W. EEG alpha and theta oscillations reflect cognitive and memory performance: A review and analysis. *Brain Res Rev*. 1999;29(2-3):169-195. doi:10.1016/S0165-0173(98)00056-3
12. Babiloni C, Frisoni GB, Pievani M, et al. White matter vascular lesions are related to parietal-to-frontal coupling of EEG rhythms in mild cognitive impairment. *Hum Brain Mapp*. 2008;29(12):1355-1367. doi:10.1002/hbm.20467
13. Babiloni C, Pievani M, Vecchio F, et al. White-matter lesions along the cholinergic tracts are related to cortical sources of eeg rhythms in amnesic mild cognitive impairment. *Hum Brain Mapp*. 2009;30(5):1431-1443. doi:10.1002/hbm.20612
14. Babiloni C, Frisoni GB, Pievani M, et al. White-matter vascular lesions correlate with alpha EEG sources in mild cognitive impairment. *Neuropsychologia*. 2008;46(6):1707-1720. doi:10.1016/j.neuropsychologia.2008.03.021
15. Loeffler M, Engel C, Ahnert P, et al. The LIFE-Adult-Study: Objectives and design of a population-based cohort study with 10,000 deeply phenotyped adults in Germany. *BMC Public Health*. 2015;15(1):691. doi:10.1186/s12889-015-1983-z
16. Lampe L, Zhang R, Beyer F, et al. Visceral obesity relates to deep white matter hyperintensities via inflammation. *Ann Neurol*. 2019;85(2):194-203. doi:10.1002/ana.25396
17. Shiee N, Bazin PL, Ozturk A, Reich DS, Calabresi PA, Pham DL. A topology-preserving approach to the segmentation of brain images with multiple sclerosis lesions. *Neuroimage*. 2010;49(2):1524-1535. doi:10.1016/j.neuroimage.2009.09.005

18. Avants BB, Tustison NJ, Song G, Cook PA, Klein A, Gee JC. A reproducible evaluation of ANTs similarity metric performance in brain image registration. *Neuroimage*. 2011;54(3):2033-2044. doi:10.1016/j.neuroimage.2010.09.025
19. Jenkinson M, Beckmann CF, Behrens TEJ, Woolrich MW, Smith SM. Fsl. *Neuroimage*. 2012;62(2):782-790. doi:10.1016/j.neuroimage.2011.09.015
20. DeCarli C, Fletcher E, Ramey V, Harvey D, Jagust WJ. Anatomical Mapping of White Matter Hyperintensities (WMH). *Stroke*. 2005;36(1):50-55. doi:10.1161/01.str.0000150668.58689.f2
21. Jawinski P, Kittel J, Sander C, et al. Recorded and reported sleepiness: The association between brain arousal in resting state and subjective daytime sleepiness. *Sleep*. 2017;40(7). doi:10.1093/sleep/zsx099
22. Bell AJ, Sejnowski TJ. An Information-Maximization Approach to Blind Separation and Blind Deconvolution. *Neural Comput*. 1995;7(6):1129-1159. doi:10.1162/neco.1995.7.6.1129
23. Hardstone R, Poil SS, Schiavone G, et al. Detrended fluctuation analysis: A scale-free view on neuronal oscillations. *Front Physiol*. 2012;3 NOV. doi:10.3389/fphys.2012.00450
24. Fischl B. FreeSurfer. *Neuroimage*. 2012;62(2):774-781. doi:10.1016/j.neuroimage.2012.01.021
25. Gramfort A, Papadopoulo T, Olivi E, Clerc M. OpenMEEG: Opensource software for quasistatic bioelectromagnetics. *Biomed Eng Online*. 2010;9. doi:10.1186/1475-925X-9-45
26. Pascual-Marqui RD. Discrete, 3D distributed, linear imaging methods of electric neuronal activity. Part 1: exact, zero error localization. October 2007. http://arxiv.org/abs/0710.3341.
27. Desikan RS, Ségonne F, Fischl B, et al. An automated labeling system for subdividing the human cerebral cortex on MRI scans into gyral based regions of interest. *Neuroimage*. 2006;31(3):968-980. doi:10.1016/j.neuroimage.2006.01.021
28. Hochberg Y. Controlling the False Discovery Rate : A Practical and Powerful Approach to Multiple Testing. *J R Stat Soc*. 2016;57(1):289-300.
29. Winkler AM, Ridgway GR, Webster MA, Smith SM, Nichols TE. Permutation inference for the general linear model. *Neuroimage*. 2014;92:381-397. doi:10.1016/j.neuroimage.2014.01.060
30. Ryu SY, Coutu JP, Rosas HD, Salat DH. Effects of insulin resistance on white matter microstructure in middle-aged and older adults. *Neurology*. 2014;82(21):1862-1870. doi:10.1212/WNL.0000000000000452
31. Tingley D, Yamamoto T, Hirose K, Keele L, Imai K. Mediation: R package for causal mediation analysis. *J Stat Softw*. 2014;59(5):1-38. doi:10.18637/jss.v059.i05
32. Stomrud E, Hansson O, Minthon L, Blennow K, Rosén I, Londos E. Slowing of EEG correlates with CSF biomarkers and reduced cognitive speed in elderly with normal cognition over 4 years. *Neurobiol Aging*. 2010;31(2):215-223. doi:10.1016/j.neurobiolaging.2008.03.025
33. Dierks T, Jelic V, Pascual-Marqui RD, et al. Spatial pattern of cerebral glucose metabolism (PET) correlates with localization of intracerebral EEG-generators in Alzheimer's disease. *Clin Neurophysiol*. 2000;111(10):1817-1824. doi:10.1016/S1388-2457(00)00427-2
34. Leunissen I, Coxon JP, Caeyenberghs K, Michiels K, Sunaert S, Swinnen SP. Task switching in traumatic brain injury relates to cortico-subcortical integrity. *Hum Brain Mapp*. 2014;35(5):2459-2469. doi:10.1002/hbm.22341
35. Smith CD, Snowdon DA, Wang H, Markesbery WR. White matter volumes and

periventricular white matter hyperintensities in aging and dementia. *Neurology*. 2000;54(4):838-842. doi:10.1212/WNL.54.4.838
36. Fields RD. White matter in learning, cognition and psychiatric disorders. *Trends Neurosci*. 2008;31(7):361-370. doi:10.1016/j.tins.2008.04.001
37. Fields RD. A new mechanism of nervous system plasticity: Activity-dependent myelination. *Nat Rev Neurosci*. 2015;16(12):756-767. doi:10.1038/nrn4023
38. Pfurtscheller G, Lopes Da Silva FH. Event-related EEG/MEG synchronization and desynchronization: Basic principles. *Clin Neurophysiol*. 1999;110(11):1842-1857. doi:10.1016/S1388-2457(99)00141-8
39. Suffczynski P, Kalitzin S, Pfurtscheller G, Lopes Da Silva FH. Computational model of thalamo-cortical networks: Dynamical control of alpha rhythms in relation to focal attention. *Int J Psychophysiol*. 2001;43(1):25-40. doi:10.1016/S0167-8760(01)00177-5
40. Sahoo B, Pathak A, Deco G, Banerjee A, Roy D. Lifespan associated global patterns of coherent neural communication. *Neuroimage*. 2020;216:116824. doi:10.1016/j.neuroimage.2020.116824
41. Scally B, Burke MR, Bunce D, Delvenne JF. Resting-state EEG power and connectivity are associated with alpha peak frequency slowing in healthy aging. *Neurobiol Aging*. 2018;71:149-155. doi:10.1016/j.neurobiolaging.2018.07.004
42. Knyazeva MG, Barzegaran E, Vildavski VY, Demonet JF. Aging of human alpha rhythm. *Neurobiol Aging*. 2018;69:261-273. doi:10.1016/j.neurobiolaging.2018.05.018
43. Mierau A, Klimesch W, Lefebvre J. State-dependent alpha peak frequency shifts: Experimental evidence, potential mechanisms and functional implications. *Neuroscience*. 2017;360(July):146-154. doi:10.1016/j.neuroscience.2017.07.037
44. Poil S-S, Hardstone R, Mansvelder HD, Linkenkaer-Hansen K. Critical-State Dynamics of Avalanches and Oscillations Jointly Emerge from Balanced Excitation/Inhibition in Neuronal Networks. *J Neurosci*. 2012;32(29):9817-9823. doi:10.1523/jneurosci.5990-11.2012
45. Nikulin V V., Brismar T. Long-range temporal correlations in electroencephalographic oscillations: Relation to topography, frequency band, age and gender. *Neuroscience*. 2005;130(2):549-558. doi:10.1016/j.neuroscience.2004.10.007
46. Smit DJA, de Geus EJC, van de Nieuwenhuijzen ME, et al. Scale-Free Modulation of Resting-State Neuronal Oscillations Reflects Prolonged Brain Maturation in Humans. *J Neurosci*. 2011;31(37):13128-13136. doi:10.1523/JNEUROSCI.1678-11.2011

Table 1 – Sample Characteristics

	Mean or n	Min.	Max.	SD
Age (in years)	69.49	60.15	80.03	4.63
Female / Male	380 / 527			
BMI (kg/m^2)	27.59	18.68	42.26	3.97
SBP (mmHg)	133.71	92.00	200.5	16.31
DBP (in mmHg)	74.54	43.5	120	9.06
Never / former / active smokers	517 / 319 / 71			
Diabetes (yes / no / unknown)	748 /143 / 16			
WMH volume (mm3)	3935	127	78509	6676.76
dWMH/pvWMH (%)	0.44	0.01	3.64	0.40
ICV (mm3)	1729811	1297219	2466529	147492.5
Mean Relative AP (%)	0.55	0.21	0.88	0.15
Mean IAPF (Hz)	9.4	7.34	12.01	0.86
Mean Scaling Exponent (ν)	0.73	0.53	1.14	0.093

Abbreviations.: AP = Alpha Power; BMI = body mass index; DBP = diastolic blood pressure; dWMH/pvWMH = the ratio of deep/periventricular white matter hyperintensities; SD = standard deviation; ICV = intracranial volume; IAPF = individual alpha peak frequency; SBP = systolic blood pressure; WMH = white matter hyperintensity

Table 2 – Positive correlation between the probability of white matter hyperintensity (WMH) occurrence and relative alpha power at EEG source space.
Peak voxel MNI coordinates (x, y, z) and cluster size (k) for the association between white matter hyperintensity probability and relative alpha power for five regions of interest for each hemisphere at source space across 855 elderly participants (TFCE, $p < 0.05$, FWE-corrected).

EEG Region	MRI Region	x	y	z	k	T-value
Left Frontal	Right Posterior Corona Radiata / Right Anterior Thalamic Radiation	21	-46	36	219	4.38
Right Cingulate	Right Anterior Thalamic Radiation / Right Anterior Thalamic Radiation	22	-49	37	2310	4.33
	Left Superior Corona Radiata	-22	6	31	655	4.29
	Right Superior Corona Radiata	29	-46	26	359	3.65
Left Cingulate	Right Anterior Thalamic Radiation / Superior Longitudinal Fasciculus	22	-49	37	3280	4.44
	Left Superior Corona Radiata	-22	6	31	597	4.33
Right Temporal	Right Anterior Thalamic Radiation	20	-50	36	4669	4.57
	Left Anterior Corona Radiata	-18	18	27	2044	4.14
	Right Inferior Fronto-occipital Fasciculus	34	-49	0	129	3.68
Left Temporal	Right Anterior Thalamic Radiation	20	-50	36	602	4.63
	Body of Corpus Callosum	16	-5	36	279	3.63
	Right Posterior Corona Radiata	19	-30	35	132	4.13
Right Parietal	Right Anterior Thalamic Radiation	20	-50	36	3983	4.72
	Left Superior Corona Radiata	-19	11	28	824	3.98
	Left Superior Longitudinal Fasciculus	-24	-12	40	210	4.12
Left Parietal	Right Superior Corona Radiata/Left Corticospinal Tract	19	-25	36	634	3.91
	Right Anterior Thalamic Radiation	20	-50	36	618	4.75
Right Occipital	Right Superior Corona Radiata	18	-19	37	8339	4.45
	Left Superior Corona Radiata	-19	9	29	1070	4.41
	Left Posterior Corona Radiata/Anterior Thalamic Radiation	-24	-27	31	100	3.94
Left Occipital	Right Superior Corona Radiata	18	-19	37	7304	4.29
	Left Superior Corona Radiata	-19	9	29	450	4.19
	Right Inferior Fronto-occipital Fasciculus	34	-37	-4	175	3.94
	Left Superior Corona Radiata	-20	-6	32	133	3.66

Table 3 – Mediation effect of total WMH volume on the association between age and relative alpha power at EEG sensor space. Significant pathways are marked in bold.

EEG Region	**frontal**		**central**		**right temporal**		**left temporal**		**parietal**		**occipital**	
	β	p or 99.5% CI	β	p or 99.5% CI	β	p or 99.5% CI	β	p or 99.5% CI	β	p or 99.5% CI	β	p or 99.5% CI
Total effect c (Age on rel. AP)	0.0004	0.742	0.0006	0.58	**0.002**	**0.03**	0.002	0.0620	0.0017	0.166	0.0006	0.584
Mediation effect a*b (Age on rel. AP via total WMH)	0.0009	[-0.0003, 0.0021]	0.001	[-0.00008, 0.0022]	**0.0013**	**[0.0003, 0.02]**	**0.0011**	**[0.00002, 0.002]**	**0.0015**	**[0.0002, 0.0028]**	**0.0014**	**[0.00012, 0.0029]**
Direct effect c' (Age on rel. AP)	-0.0005	0.721	-0.0004	0.73	0.0008	0.44	0.0009	0.3944	0.0002	0.894	-0.0008	0.557

Abbreviations.: rel AP = Relative Alpha Power; CI = Confidence Interval; WMH = White matter hyperintensity

Figure Legends

Figure 1 – Flow chart visualizing the selection process of the MRI and EEG sample.

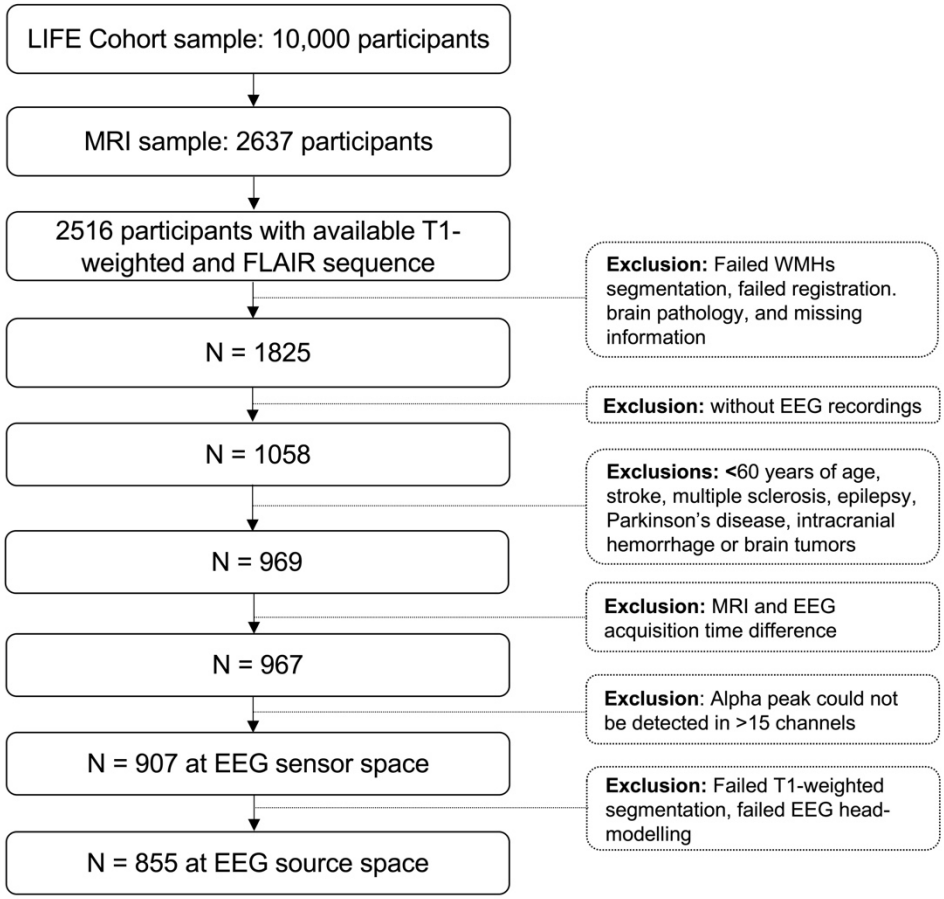

Figure 2 – Illustration of the regions of interest (ROIs) identified for EEG.

Schematic topography for resting state EEG in **A)** sensor space and **B)** source space. ROIs that form the frontal region are in purple, central region and cingulate region (source) in orange, temporal region in yellow, parietal region in green, and occipital region in blue.

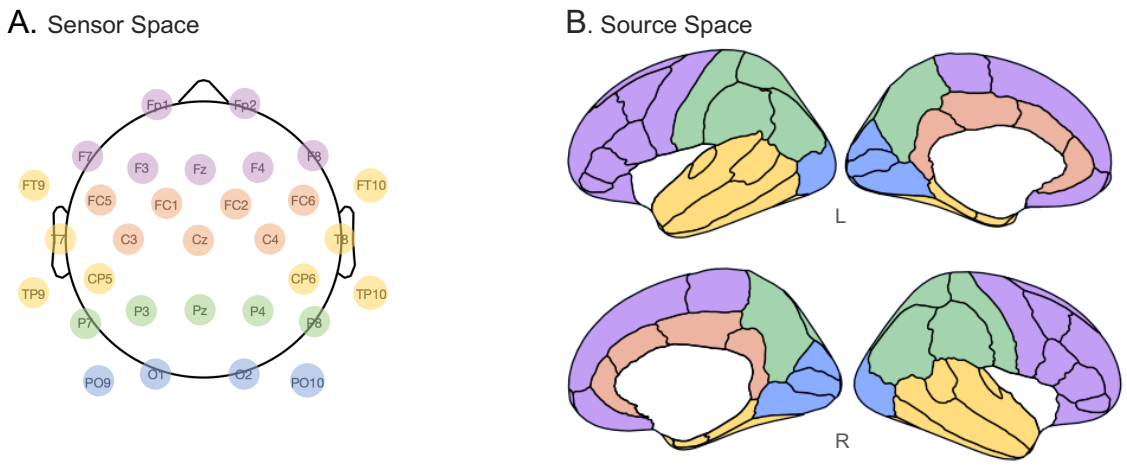

Figure 3 – Illustration of parameters of alpha oscillations.

A) Resting state EEG time series data (blue) consists of various frequency bands that can be defined by their power and peak frequency. **B)** The temporal dynamics of a signal filtered in alpha frequency range (8–12 Hz) is assessed by the properties of its amplitude envelope (red) using long-range temporal correlations (LRTC). Scaling exponent (ν) quantifies the presence of LRTC.

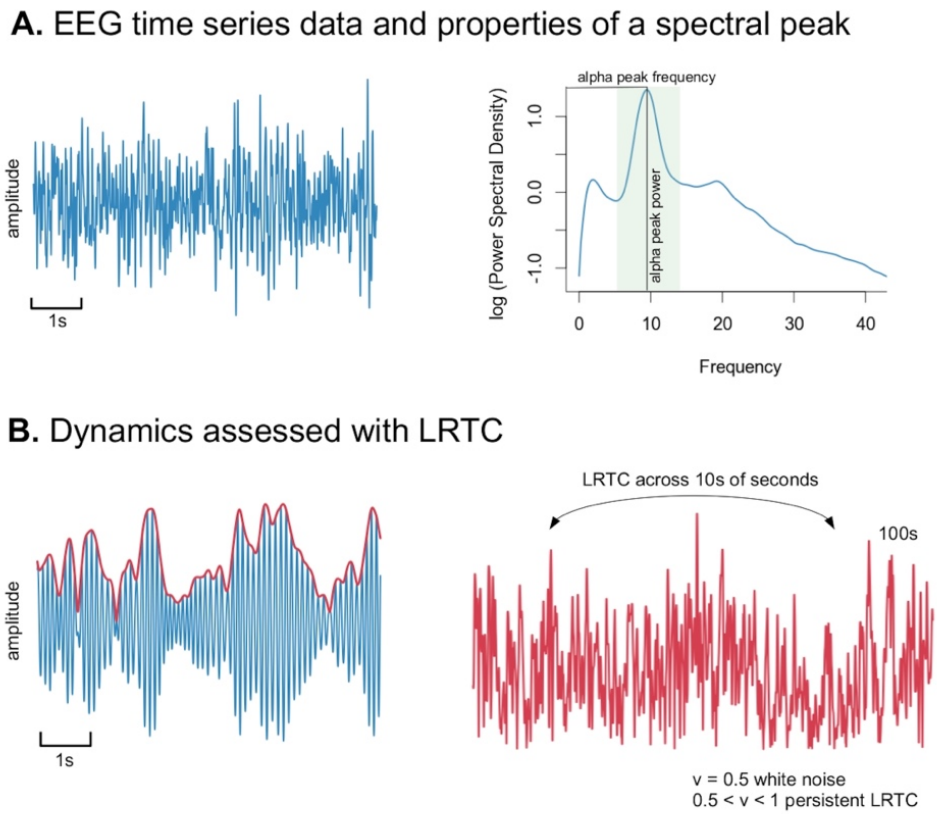

Figure 4 – Association between regional white matter hyperintensities (WMHs) and relative alpha power at EEG sensor space.
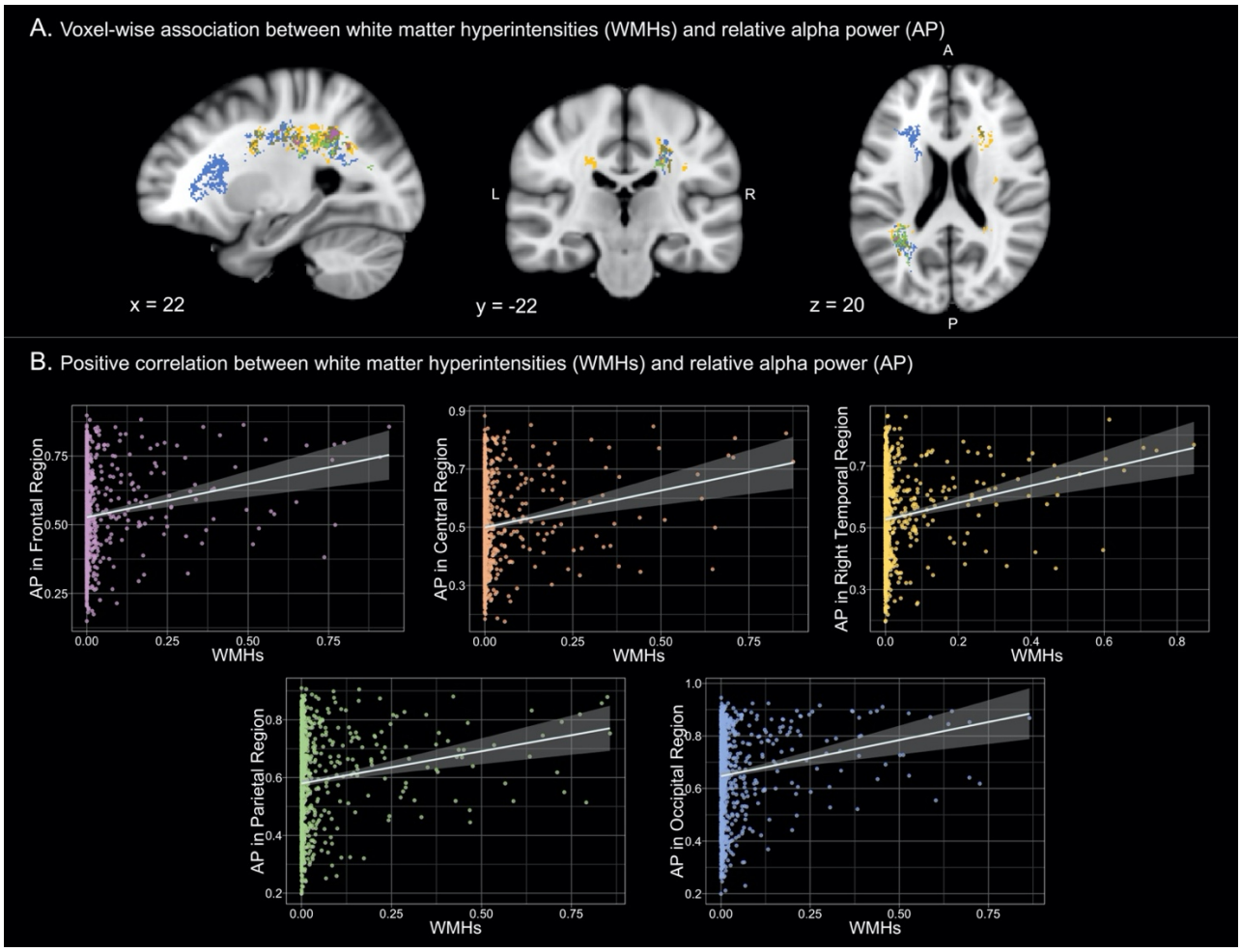
A) Voxel-wise correlation between probability of WMH occurrence and relative alpha power in the EEG frontal region (purple), central region (orange), right temporal region (yellow), parietal region (green), and occipital region (blue). The significant clusters based on whole-brain voxel-wise inference analyses (TFCE, FWE-corrected, $p < 0.05$). **B)** Scatter plots show the positive association between relative alpha power. The resulting statistical images (P-map) were further thresholded at 0.05 and binarized. Abbreviations.: A = anterior; L = left; R = right; P = posterior